Novel Catalytic Non-Thermal Plasma Reactor for the Destruction of Volatile Organic Compounds

L. Kiwi-Minsker*, Ch. Subrahmanyam, A. Renken
Ecole Polytechnique Fédérale de Lausanne (GGRC-EPFL), CH-1015 Lausanne, Switzerland, Fax: +41-21- 693 31 90, lioubov.kiwi-minsker@epfl.ch

Abstract

A novel dielectric barrier discharge (DBD) reactor has been designed as catalytic non-thermal plasma (NTP) reactor. It was tested for the abatement of diluted volatile organic compounds (VOCs) of different nature. The novelty of the DBD reactor is that a metallic catalyst made of sintered metal fibers (SMF) also acts as the inner electrode. The SMF electrodes modified with oxides of Ti, Mn and Co were efficient during the destruction of selected VOCs of different nature like toluene, isopropanol (IPA) and trichloroethylene (TCE). It has been observed that at a fixed concentration of VOC, total oxidation of IPA was achieved at lower specific input energy (SIE) compared to toluene and TCE. Among the catalysts studied, MnO_x/SMF showed the best performance, probably due to the formation of active oxygen species by *in-situ* decomposition of ozone on the catalyst surface. The SMF electrode modified with MnO_x and TiO_2 catalyst effectively destroys TCE due to the synergy between plasma excitation of the TCE molecules and their catalytic oxidation. The latter process was further enhanced by photocatalysis, since TiO_2 absorbs the UV light produced by the NTP.

Keywords: Non-thermal Plasma, dielectric barrier discharge, VOC abatement, plasma photocatalysis, sintered metal fibers

* Corresponding author

1. Introduction

The emission of volatile organic compounds (VOCs) by various industrial and automobile sources into the atmosphere is an important source of air pollution and social concern as VOCs are precursors of photochemical oxidants and suspended particulate matter (SPM) that give adverse impact on the human health. Therefore, abatement of VOCs is an important issue that has to be handled through highly efficient low cost processes. For the abatement of dilute VOCs (≤1000 ppm), conventional techniques like thermal and thermocatalytic oxidation are not suitable mainly due to high energy demand [1-5]. Among the alternatives, non-thermal plasma (NTP) generated at atmospheric pressure seems to be advantageous. The plasma, also called the fourth state of the matter, is characterized by ionization of a gas giving a wide range of species such as energetic electrons, radicals, ions and excited species as well as radiation [6]. In NTP, the electrical energy is primarily used for the production of energetic electrons without heating the flue gas. In dielectric barrier discharge (DBD), the presence of a dielectric distributes the microdischarges throughout the discharge volume. These microdischarges initiate chemical reactions in the gas phase through electron impact dissociation and ionization of

the carrier gas [7-9]. However, NTP abatement of VOCs shows low selectivity (0.3 to 0.5) to total oxidation (CO_2 and H_2O), resulting undesired and sometimes toxic by-products like CO, O_3, NO_x and partially oxidized hydrocarbons [10]. In order to improve the efficiency of NTP, catalytic plasma technique has been proposed, where the catalyst can be either placed in discharge zone (*in*-plasma catalytic reactor or plasma driven catalysis) or downstream to discharge zone (*post*-plasma catalytic reactor or plasma enhanced catalysis). Even though *in*-plasma configuration was found to be promising for the abatement of VOCs, deactivation of the catalyst by solid carbon deposits limits the application of this technique. To some extent, deactivation can be minimized by placing the catalyst downstream to plasma zone. A better performance with a *post*-plasma catalytic treatment has been reported [1,5,11]. However, contrary to *in*-plasma technique, where short-lived plasma species promote the reaction, during *post*-plasma catalytic process, oxidation of effluents is mainly due to long-lived species like ozone and oxides of nitrogen [12]. Therefore, a synergy between plasma excitation and catalysis is expected only when the catalyst is placed in discharge [13,14]. Hence, there is a need for a new configuration of plasma catalytic reactors to use the potentials of *in*-plasma catalytic treatment.

Recently, we reported a novel DBD reactor, where the inner electrode made of sintered metal fiber (SMF) filters also acts as the catalyst [15, 16]. The SMF electrode was modified by transition meal oxides in order to improve the efficiency of plasma reaction. During the present study, abatement of model VOCs having different nature like toluene, isopropanol (IPA) and trichloroethylene (TCE) was tested to evaluate the performance of the catalytic DBD reactor. Influence of applied voltage, frequency, ozone and the ultraviolet light (UV) produced in the discharge on the performance of DBD reactor was also studied.

2. Experimental

2.1. Materials & catalyst preparation.

Sintered metal fibers filters (Southwest Screens & Filters SA, Belgium) made of stainless steel consists of thin uniform metal fibers (Ø-40 μm) and has a wetness capacity of ~ 30 wt %. For the preparation of 3wt % MnO_x and CoO_x on SMF, the stainless steel filters were oxidized at 873 K for 3h, followed by impregnation with Co and Mn nitrate aqueous solutions of desired concentration. TiO_2/SMF and TiO_2/MnO_x/SMF were prepared by precipitation of Ti-(IV) bis (ammonium lactato) dihydroxide, 50-wt% solution in water. Drying at room temperature followed by calcination in air at 773 K for 5 h results in catalytic electrodes of metal oxide supported on SMF. The TiO_2, CoO_x and MnO_x /SMF contains 3 wt% of the metal oxide, whereas TiO_2/MnO_x/SMF contains 1 and 3 wt% of TiO_2 and MnO_x, respectively. XPS analysis confirmed the formation of metal oxides on SMF, whereas transmission electron microscopy coupled with diffraction pattern confirms the formation of titania anatase [17]. Finally, SMF filters were subjected to an electrical hot press to shape them into cylindrical form.

2.2. Experimental set-up and procedure

The experimental set-up consisted of a motor driven syringe pump for the introduction of VOC, which was mixed with air (500 ml/min (STP) for toluene, IPA and 700 ml/min for TCE) and was fed into the plasma reactor with a Teflon tube. VOC

concentration at the outlet of the reactor was measured with a gas chromatograph (Shimadzu 14 B) equipped with a FID and a SP-5 capillary column. The formation of CO_2 and CO was simultaneously monitored with an infrared gas analyzer (Siemens Ultramat 22), whereas ozone formed in the plasma reactor was measured with an UV absorption ozone monitor (API-450 NEMA). The emission spectrum of the discharge at 20 kV was measured with a SM- 240 spectrometer (CVI Spectral Products) with a Sony ILX511 CCD linear array detector.

As the volume changes due to chemical reactions are negligible, selectivity of CO_2 and CO_x was defined as

$$S_{CO}(\%) = \frac{[CO]}{x \cdot ([VOC]_0 - [VOC])} * 100$$

$$S_{CO2}(\%) = \frac{[CO_2]}{x \cdot ([VOC]_0 - [VOC])} * 100$$

$$S_{COx} = S_{CO} + S_{CO2}$$

where X= 7, 3 and 2 for Toluene, IPA and TCE, respectively.

2.3. Plasma reactor and power supply

A detailed description of the DBD reactor was reported elsewhere [15]. Briefly, the dielectric discharge was generated in a cylindrical quartz tube with an inner diameter of 18.5 mm. A silver paste painted on the outer surface of the quartz tube acts as the outer electrode, whereas a modified SMF was used as the inner electrode (Fig. 1). The SMF was modified by supporting Ti, Mn and Co oxides on the filter surface. The discharge length was 10 cm and discharge gap was fixed at 3.5 mm during the destruction of toluene and IPA, whereas it was varied between 3.5 to 1.25 mm for TCE. One end of SMF filter was connected to AC high voltage through a copper rod, whereas the other end was connected to the inlet gas stream through a Teflon tube. The specific input energy (SIE) in the range 160-1650 J/l was applied by varying the AC high voltage (12.5-22.5 kV) and frequency (200-350 Hz). Conversion of VOC at each voltage was measured after 30 min. A V-Q Lissajous method was used to determine the discharge power (W) in the plasma reactor, where the charge Q (i.e. time integrated current) was recorded by measuring the voltage across the capacitor of 220 nF connected to the ground electrode. The voltage was measured with a high voltage probe (Luke 80 K-40 HV). The signals of V and Q were recorded with a digital oscilloscope (Tektronix, TDS 3054) and plotted to get a typical V-Q Lissajous diagram as shown in Fig. 2.

3. Results

3.1. Specific input energy (SIE)

Figure 2 represents a typical V-Q Lissajous figure for 22.5 kV, 17.5 kV and 12.5 kV at a frequency of 200 Hz for a discharge gap of 1.25 mm. The area of the Lissajous figure characterizes the energy dissipated during one period of the voltage. The average power (W) in the discharge was calculated by multiplying the area by the frequency and the capacitance. The specific input energy (SIE) of the discharge was calculated using the relation:

SIE (J/l) = power (W) / gas flow rate (l/s).

As seen from the Fig. 2, with increasing applied voltage, power increases and thereby SIE. For example, at 200 Hz for a discharge gap of 3.5 mm, the SIE increased from 160 J/l (12.5 kV) to 295 J/l (22.5 kV). When the frequency was increased to 300 Hz, a considerable increase of SIE up to 1030 J/l was observed. When the frequency was further increased to 350 Hz, the SIE reached a maximum of 1650 J/l at 22.5 kV.

3.2. Discharge characterization

It is known that NTP reactors operated in air produce ultra violet (UV) light, which comes from the excited nitrogen molecules. Earlier attempts combining NTP with a TiO_2 photocatalyst to abate VOCs indicate that the contribution of photocatalysis induced by UV light from the plasma was not significant [18]. In addition, the improvement in the activity was attributed only due to surface activation of TiO_2 by discharge plasma. Nevertheless, the position of the photocatalyst should be optimized to utilize the UV light emitted by NTP. During the destruction of TCE with TiO_2 /SMF electrodes, the effect of the UV light can be expected only if NTP emits radiation in the range $\lambda \leq$ 370-380 nm, which is equivalent to the band gap of anatase (3.2 eV). During the present study, emission spectrum of the discharge (Fig. 3) in the wavelength range 250-500 nm confirms the presence of UV light originated from excited nitrogen molecules (N_2^*). The high-energy electrons generated in the plasma excite and ionize the nitrogen molecules leading to the N_2 ($C^3\Pi_u$) and N_2^+ ($B^2\Sigma_u^+$) electronic states. De-excitation of these states occurs due to radiative emission and molecular quenching. Hence, decay of $C^3\Pi_u$ state to $B^3\Pi_g$ (N_2, $C^3\Pi_u \rightarrow B^3\Pi_g$) induces second positive system (SPS) with the most intense band corresponding to (0-0) transition at 337 nm. Similarly, decay of $B^2\Sigma_u^+$ state towards $X^2\Sigma_g^+$ (N_2^+, $B^2\Sigma_u^+ \rightarrow X^2\Sigma_g^+$) results first negative system (FNS) corresponding to (0-0) transition at 391 nm [19,20]. Therefore, the emission from excited nitrogen molecules (N_2^*) is in the range of the band gap of TiO_2 catalyst.

3.3. Abatement of toluene in the catalytic NTP reactor

Conversion of toluene (100 ppm) diluted by air was followed by varying the applied voltage between 12.5 to 22.5 kV at a constant frequency of 200 Hz, corresponding to the SIE values 160 and 295 J/l, respectively. The inner electrode was either a conventional Cu electrode, or the catalytic SMF electrode. As seen from the Fig.4a, SMF electrode showed the same activity as that of Cu electrode. With SMF electrode, conversion increases with increasing applied voltage reaching ~100% at 20 kV (265 J/l). Interestingly, with CoO_x and MnO_x/SMF catalytic electrodes, ~100 % conversion of toluene was achieved even at 17.5 kV that corresponds to SIE of 235 J/l.

Figure 4b represents the selectivity to CO_x during destruction of 100 ppm of toluene. Selectivity to CO_x also increases with increasing voltage and reaches 100 % (no carbon deposit) on all catalysts when the voltage was higher than 17.5 kV that corresponds to SIE of 235 J/l. Figure 4b also represents the selectivity to CO_2 for various catalysts during destruction of 100 ppm of toluene. As seen from the Fig.4b, SMF showed only ~50 % selectivity to CO_2 at 295 J/l, whereas MnO_x/SMF shows better performance, where the selectivity to CO_2 was ~ 80 % even at 235 J/l (17.5 kV). It is worth mentioning that with MnO_x/SMF catalyst, at 17.5 kV, the conversion was ~100% (Fig. 4a) and there was no polymeric carbon deposit (Fig. 4b). Hence, the novel DBD reactor with catalytic SMF electrode showed remarkable activity during the destruction

of toluene. The better performance of CoO_x and MnO_x/ SMF is due to the formation of atomic oxygen by "*in*-situ" decomposition of ozone on the surface of the catalytic electrode [15].

Since MnO_x/SMF showed better performance, total oxidation of 250 ppm of toluene was studied as a function of SIE varied in the range 160 to 1650 J/l by changing the voltage (12.5 to 22.5 kV) and frequency (200-350 Hz). Typical results indicate that ~100 % destruction of 250 ppm of VOCs was achieved at SIE < 250 J/l [16]. When SIE was varied in the range 160-295 J/l (i.e. frequency 200 Hz), the maximum selectivity to CO_2 was around 65 % at 295 J/l. With increasing SIE up to 740 J/l (17.5 kV, 350 Hz), the CO_2 selectivity reached ~ 80%. Close to 100 % selectivity to CO_2 can be obtained by further increasing SIE up to 1650 J/l. It can be concluded that for an initial toluene concentration of 250 ppm, by operating at a threshold SIE value of 740 J/l, a high selectivity (~80 %) towards CO_2 can be achieved.

3.3. Abatement of isopropanol in the catalytic NTP reactor

Isopropanol (IPA) is one of the solvents used in electronic industry for cleaning the printed circuit boards and LCD monitors. IPA from industrial effluent can be recovered by adsorption into water using wet scrubbers followed by distillation or pervaporation. Thermal oxidation of alcohols needs temperature in the range 873 to 973K, whereas thermocatalytic oxidation takes place in the temperature range 523-673K. However, these techniques are not suitable for the abatement of diluted alcohols. The NTP technique has already been tested for the destruction of IPA, however, formation of acetone as a stable secondary product was observed. Abatement of acetone demands a high energy (~1000 J/l), which is not energetically favorable. During the present study, oxidation of 100 ppm of IPA over catalytic SMF electrodes has been investigated. Like in the case of toluene, at any SIE, metal oxide supported SMF electrodes showed better activity compared to SMF non-modified electrode (Fig.5a). With the SMF electrode, the IPA conversion reaches ~ 100% only at 22.5 kV (295 J/l), whereas with Co and Mn oxides supported SMF electrodes, it was achieved at 15 kV that corresponds to SIE of 195 J/l. Figure 5b shows the selectivity to CO_x during the destruction of 100 ppm of IPA in the range of SIE 160 to 295 J/l. As seen, with SMF electrode, selectivity to CO_x reaches ~ 100% at voltage higher than 20 kV (265J/l), whereas with CoO_x and MnO_x/SMF electrodes this was achieved at 235 J/l. The selectivity to CO_2 also followed the same trend. MnO_x/SMF showed ~100% CO_2 selectivity at 265 J/l, whereas under the same experimental conditions, non-modified SMF showed only ~50% selectivity. As explained above, formation of atomic oxygen by "in-situ" decomposition of ozone on the surface of catalytic MnO_x/SMF electrode shifted the product distribution towards total oxidation. Hence, with the novel DBD reactor with the catalytic MnO_x/SMF electrode, total oxidation of alcohol (100 ppm IPA in air) was achieved at 265 J/l. MnO_x/SMF was tested during the abatement of 250 ppm of IPA in the SIE range 160 to 760 J/l and typical results indicate that ~100% conversion of IPA was achieved at SIE ≤ 250 J/l, whereas, total oxidation was achieved at 760 J/l.

3.4. Abatement of trichloroethylene in the catalytic NTP reactor

Chlorinated organic compounds, especially trichloroethylene (TCE) are effective washing agents to remove hydrophobic contaminants [2]. Photocatalytic decomposition

of chlorinated hydrocarbons has been traditionally used for its abatement. However, catalytic and photocatalytic methods for the abatement of TCE produce toxic by-products like phosgene. Non-thermal plasma in air produces ultra violet (UV) light, which comes from the excited nitrogen molecules. Attempts were done to combine NTP with a photocatalyst TiO_2 for the destruction of VOCs [14, 18, 20]. However, the results indicate that the contribution of photocatalysis induced by UV light from plasma was not significant. In addition, the improvement in the activity was attributed to the surface activation of TiO_2 by discharge plasma [18, 20]. During the present study, abatement of diluted TCE (250 ppm in air) was tested by using the DBD reactor with catalytic SMF electrode modified with TiO_2, MnO_x and TiO_2/MnO_x. Since the formation of ultraviolet light in the wavelength range 200-500 nm has been confirmed (Fig. 2), the SMF modified with TiO_2 anatase has been used to study the influence of UV light on the performance of the DBD reactor.

Efficiency of the modified catalytic SMF electrodes was tested during the destruction of 250 ppm of TCE for a discharge gap of 1.25 mm as a function of SIE, which was varied in the range 140 to 1100 J/l by changing the voltage (12.5 to 22.5 kV) at 250 Hz. The results are presented in Fig. 6. Throughout the range of the SIE applied, starting from 140 J/l, ~ 100% conversion of TCE was achieved. However, during the abatement of VOCs, the desired is the total oxidation of avoiding the formation of undesired products like CO and polymeric carbon deposit that deactivates the catalyst. Figure 6 represents the selectivity profile of the gaseous products formed over SMF electrodes. With non-modified SMF electrode at 140 J/l (12.5 kV and 250 Hz), the selectivity to COx is only ~ 55 %, and 45% towards unidentified polymeric carbon deposit. However, formation of phosgene was not observed. The selectivity to CO_x increases to ~ 100 % with increasing SIE to ~ 1100 J/l.

Figure 6 also presents the selectivity to CO_2, showing the effect of the metal oxide modification. As seen from the Fig. 6, at 140 J/l (12.5 kV), the SMF electrode showed only ~5 % selectivity to CO_2, which was increased only up to ~ 20 % at 1100 J/l (22.5 kV). However, at any SIE, the metal oxide modified electrodes showed higher CO_2 selectivity. The selectivity to CO_2 follows the order TiO_2/MnO_x/SMF (80%) > MnO_x/SMF (65%)> TiO_x/SMF (40%) >SMF (25%). Interesting is that the TiO_2 modified SMF also showed higher CO_2 selectivity than the SMF electrode. Even at 140 J/l, the TiO_2/SMF showed ~ 15 % selectivity to CO_2 against ~ 5% on the SMF. With increasing SIE to 1100 J/l (22.5 kV), the selectivity to CO_2 increases up to ~ 40%, whereas, under these experimental conditions the SMF shows only 20% selectivity. The better performance of TiO_2 over SMF could be either due to "in-situ" decomposition of ozone or the influence of UV light formed in the discharge on the anatase photocatalyst.

In order to ensure the plausible mechanism of TCE destruction, ozone concentration at the outlet of the reactor was measured. At 575 J/l (17.5 kV), with SMF and TiO_2/ SMF, the formation of 750 and 800 ppm of ozone was observed, respectively. When MnOx and TiO_2/MnO_x/SMF electrodes were used, the ozone concentration decreased to ~ 0 ppm. It clearly indicates that the improvement observed with MnO_x modified electrodes might be due to "in-situ" decomposition of ozone that leads to the formation of strong oxidant (atomic oxygen). Like-wise, the thermal activation of TiO_2 catalyst requires a temperature in the range 573 to 673 K, whereas, during the present study, the outlet gas temperature never exceeded ~ 310K. Hence, the better performance

of TiO_2/SMF over SMF cannot be attributed to the thermal activation of TiO_2. The improvement in the activity may be due to the influence of UV light coming from NTP. In order to confirm this observation, MnO_x/SMF was modified with TiO_2, and the resulting catalytic electrode as seen from the Fig. 6, increased the CO_2 selectivity to ~ 80% against ~65 % with MnO_x/SMF. This improvement was assigned to the synergy between plasma excitation of the molecules and their catalytic oxidation. The latter process was further enhanced by photocatalysis, since TiO_2 absorbs the UV light produced by NTP.

3.5. Discussion

The novelty of the DBD reactor presented in this study is the use of catalytic SMF electrode as the inner electrode. From the data presented above, the main advantage of using catalytic SMF electrode is a high selectivity to CO_2 at low input energy and the minimization of undesired C-solid deposit. During the destruction of VOCs, the better performance of MnO_x/SMF over others may be due to *in-situ* decomposition of ozone leading to the formation of active oxygen atoms (O^*) on the catalyst surface [13, 16]. It was earlier reported that on MnO_x surface, a part of the atomic oxygen O^* is present in the form of O (^3P) [13]. The formation and stabilization of O (^3P) species on the MnO_x/SMF may be responsible for the better performance of the plasma reactor. The reported DBD reactor with the catalytic electrode also minimizes the carbon deposit diminishing the deactivation. During the destruction of TCE, TiO_2 modified SMF electrodes improved the selectivity to total oxidation which was assigned due to the influence of UV light formed in the discharge. When the TiO_2 anatase semiconductor is irradiated with UV light with energy higher than the band gap (~ 3.2 eV, $\lambda \leq 380$ nm), excitation of a valance band electron into the conduction band takes place leaving a hole in the valance band. Both the hole and the photoelectron migrate to the TiO_2 surface, where either they recombine or participate in redox reactions with adsorbed species like H_2O and O_2. The hole oxidizes adsorbed water to hydroxyl radical, whereas, the photoelectron reduces O_2 to superoxide. With the catalytic TiO_2 electrodes, NTP decomposes TCE into several intermediates, which will be adsorbed on the TiO_2 surface. These intermediates will be oxidized by the hydroxyl radical and superoxide. During the destruction of TCE, TiO_2/MnO_x/SMF showed the best performance that was assigned to the synergy between plasma excitation of the TCE molecules and their catalytic oxidation. This was further enhanced by photocatalysis, since TiO_2 absorbs the UV light produced by the NTP. Hence, it can be concluded that during the NTP abatement of VOCs, performance of catalytic plasma reactor can be improved with a suitable modification of catalytic SMF electrode.

4. Conclusions

A novel catalytic Non-Thermal Plasma (NTP) reactor with a metallic SMF electrode also functioning as a catalyst was designed. The emission spectrum of the discharge confirms the ultraviolet light, whereas XPS and TEM confirm the formation of metal oxides. The NTP reactor has been tested for the destruction of VOCs of different nature demonstrating high efficiency at low specific input energy. During the destruction of toluene and isopropanol, MnO_x/SMF showed the best performance, which was attributed to the formation of atomic oxygen by “in-situ” decomposition of ozone on the

catalyst surface. The selectivity to CO_2 during TCE destruction at a discharge gap of 1.25 mm was improved up to ~ 80 % at 1100 J/l by modifying MnO_x/SMF with TiO_2. This improvement was assigned to the synergy between plasma excitation of the TCE molecules and their catalytic oxidation. This was further enhanced by photocatalysis as TiO_2 absorbs the UV light produced by the NTP. To conclude, the NTP catalytic reactor is efficient for the abatement of VOCs at lower consumption of energy compared to thermocatalytic methods, but the reactor still needs to be optimized for achieving the total oxidation at low SIE.

Acknowledgements
The authors thank the Swiss National Science Foundation for the financial support within the SCOPES program. Technical assistance of Mr. Edy Casali, Mr. Andre Fattet, and Mr. Xanthopoulos at the EPFL is highly appreciated.

References

[1]. Magureanu, M., Mandache, N.B., Eloy, P., Gaigneaux, E.M. and Parvulescu, V. I., (2005) Appl. Catal. B: Environ., *61*, 13.
[2]. Urashima, K., and Chang, J.S., (2000) IEEE Trans. Ind. Appl., *7*, 602.
[3]. Francke, K.P., Miessner, H. and Rudolph, R., (2000) Plasma Chem. Plasma Process., *20*, 393.
[4]. Roland, U., Holzer, F. and Kopinke, F.D., (2005) Appl. Catal.B: Environ., *58*, 217.
[5]. Ayrault, C., Barrault, J., Blin-Simiand, N., Jorand, F., Pasquiers, S., Rousseau, A. and Tatibouet, J.M.,(2004) Catal. Today, *89*, 75.
[6]. Kogelschatz, U., (2003) Plasma Chem. Plasma Process., *23*, 1.
[7]. Yamamoto, T., Mizuno,K., Tamori, I., Ogata, A., Nifuku, M., Michalska, M. and Prieto, G., (1996) IEEE Trasns. Ind. Appl., *32*, 100.
[8]. Penetratnte, B., Hsiao, M.C., Bardsley, J.N., Merrit, B.T., Vogtlin, G.E., Kuthi, A., Burkhart, C.P. and Bayless, J.R., (1997) Plasma Sources Sci. Technol., *6*, 251.
[9]. Eliasson, B. and Kogelschatz, U., (1991) IEEE Trans. Plasma Sci., *19*, 1063.
[10]. Roland, U., Holzer, F. and Kopinke, F.D., (2002) Catal. Today, *73*, 315.
[11]. Roland, U., Holzer, F. and Kopinke, F.D., (2005) Appl. Catal.B: Environ., *58*, 227.
[12].Ogata, A., Mizuno, K., Kushiyama, S. and Yamamoto, T., (1999) Plasma Chem. Plasma Process., *19*, 383.
[13]. Futamura, S., Einaga, H., Kabashima, H. and Jwan, L.Y., (2004) Catal. Today, *89*, 89.
[14]. Kim, H.H., Oh, S. M., Ogata, A. and Futamura, S., (2005) Appl. Catal. B: Environ., *56*, 213.
[15]. Subrahmanyam, Ch., Magureanu, M., Renken A. and Kiwi-Minsker, L., (2006) Appl. Catal. B: Environ., *65*, 150.
[16]. Subrahmanyam, Ch., Renken A. and Kiwi-Minsker, L.,(2006) Appl. Catal. B: Environ., *65*, 157.
[17]. Subrahmanyam, Ch., Magureanu, M., Laub, D., Renken A. and Kiwi-Minsker, L., (2007) J. Phys. Chem. C., *111*, 4315.
[18]. Ogata, A., Kim, H.H., Futamura, S., Kushiyama, S. and Mizuno, K.,(2004) Appl. Catal. B: Environ., *53*, 175.
[19]. Spyrou, N. and Manassis, C., (1989) J. Phys.D : Appl. Phys., *22*, 120.
[20]. Kim, H. H., Lee, Y.H., Ogata, A. and Futamura, S., (2003) Catal. Commun., *4*, 347.

Legend to Figures

Fig. 1. Schematic presentation of the catalytic NTP reactor
Fig. 2. V-Q Lissajous figure
Fig. 3. Emission spectrum of the discharge (1.25 mm discharge gap, 20 kV and 250 Hz)
Fig. 4. Influence of specific input energy and SMF modification during the destruction of toluene on a) conversion (b) selectivity to CO_x (100 ppm, 12.5 -22.5 kV and 200 Hz)
Fig. 5. Influence of specific input energy and SMF modification during the destruction of isopropanol on a) conversion (b) selectivity to CO_x (100 ppm, 12.5 -22.5 kV and 200 Hz)
Fig. 6. Influence of specific input energy and SMF modification on the selectivity to CO_x during destruction of trichloroethylene (250 ppm, 12.5 -22.5 kV and 250 Hz)

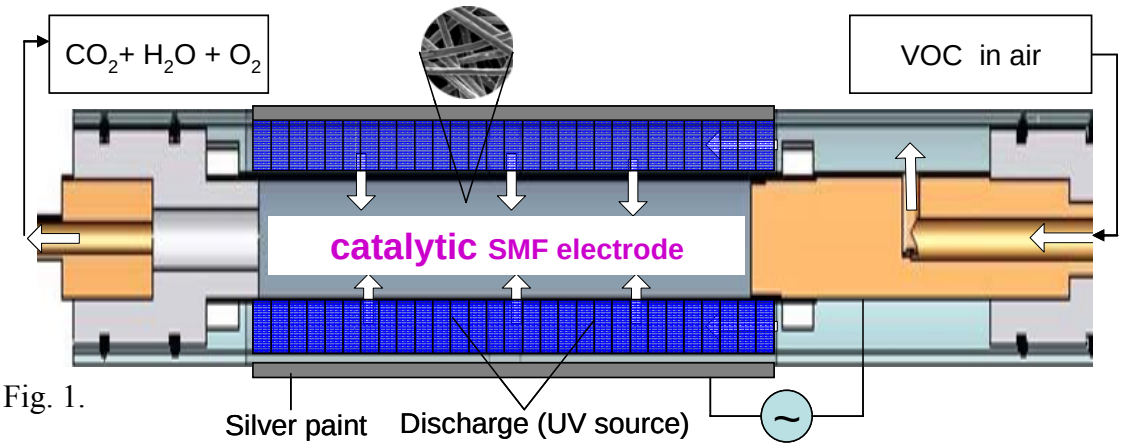
CO_2+ H_2O + O_2
VOC in air
catalytic SMF electrode
Silver paint
Discharge (UV source)
~

Fig. 1.

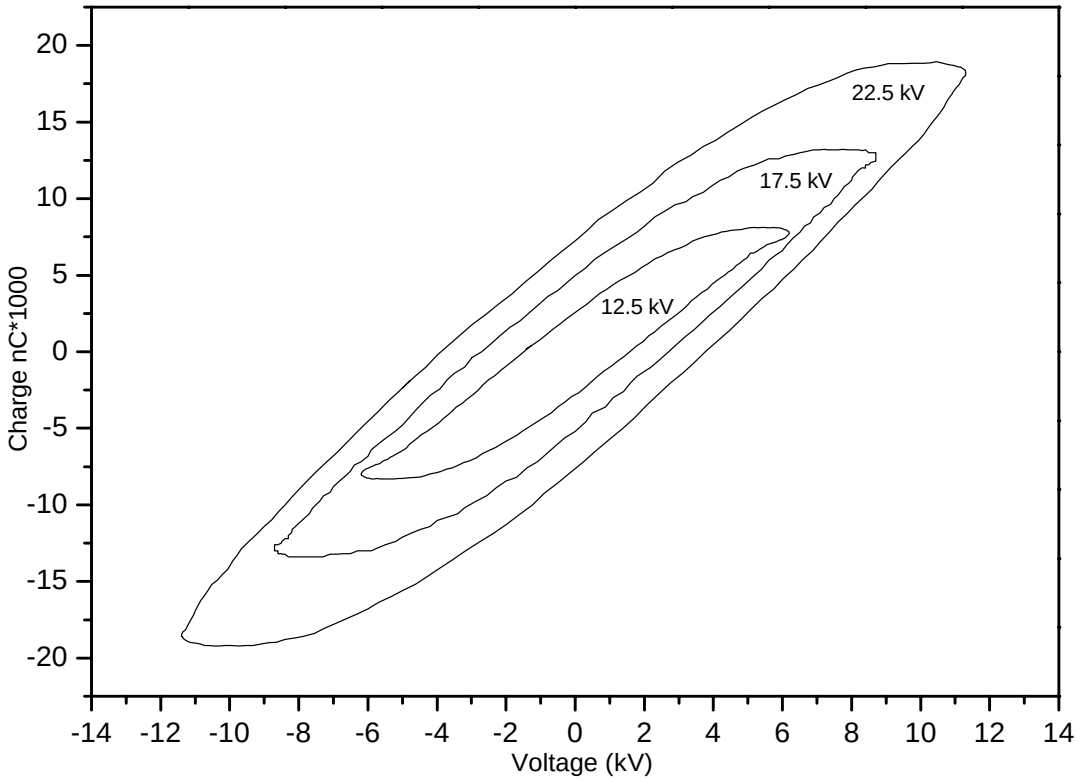
22.5 kV
17.5 kV
12.5 kV
Charge nC*1000
Voltage (kV)
20
15
10
5
0
-5
-10
-15
-20
-14
-12
-10
-8
-6
-4
-2
0
2
4
6
8
10
12
14

Fig. 2.

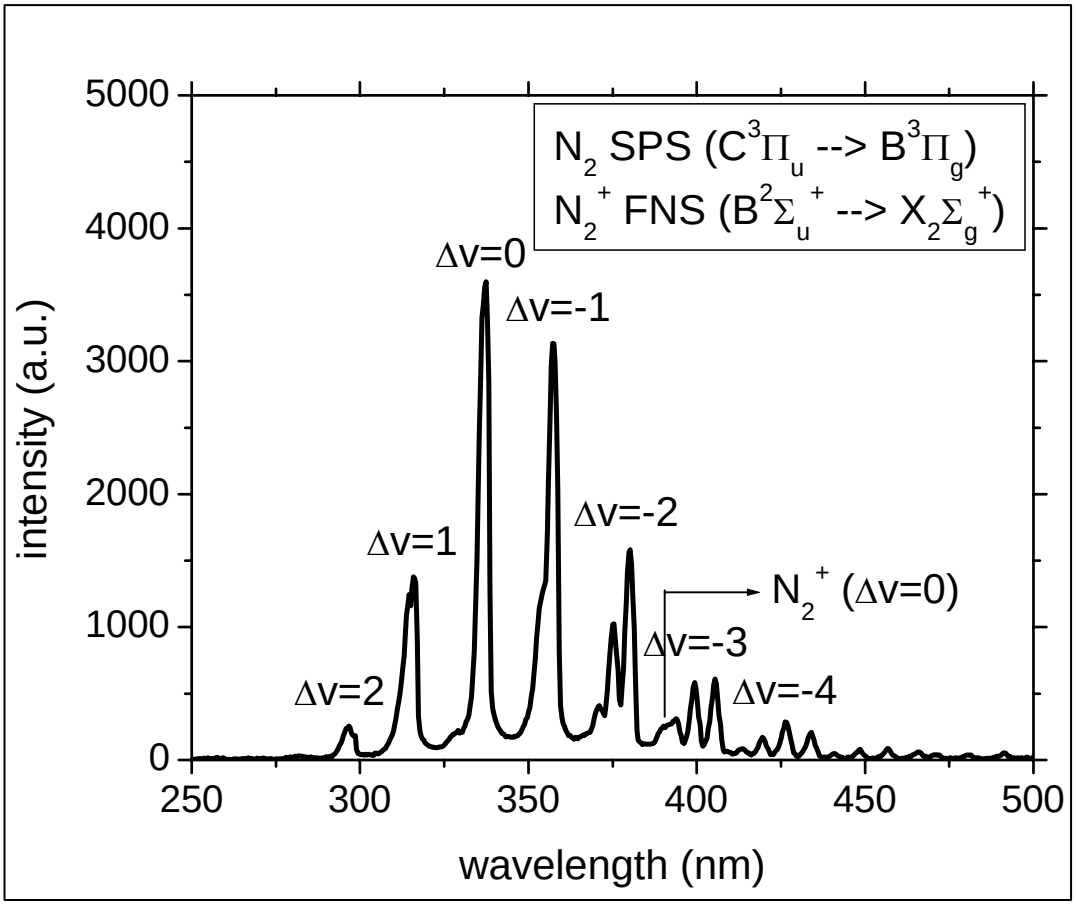
N2 SPS (C3Πu --> B3Πg)
N2+ FNS (B2Σu+ --> X2Σg+)
Δv=0
Δv=-1
Δv=-2
Δv=1
Δv=2
Δv=-3
Δv=-4
N2+ (Δv=0)
intensity (a.u.)
wavelength (nm)
0
1000
2000
3000
4000
5000
250
300
350
400
450
500

Fig. 3.

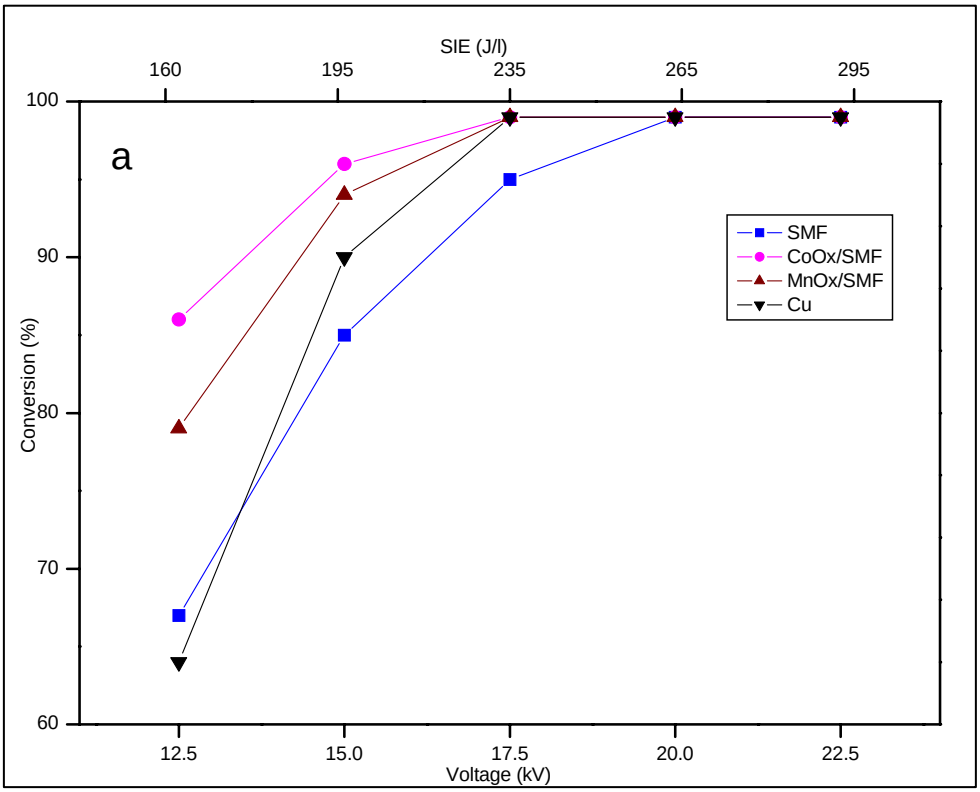
SIE (J/l)
160
195
235
265
295
100
90
80
70
60
a
Conversion (%)
SMF
CoOx/SMF
MnOx/SMF
Cu
12.5
15.0
17.5
20.0
22.5
Voltage (kV)

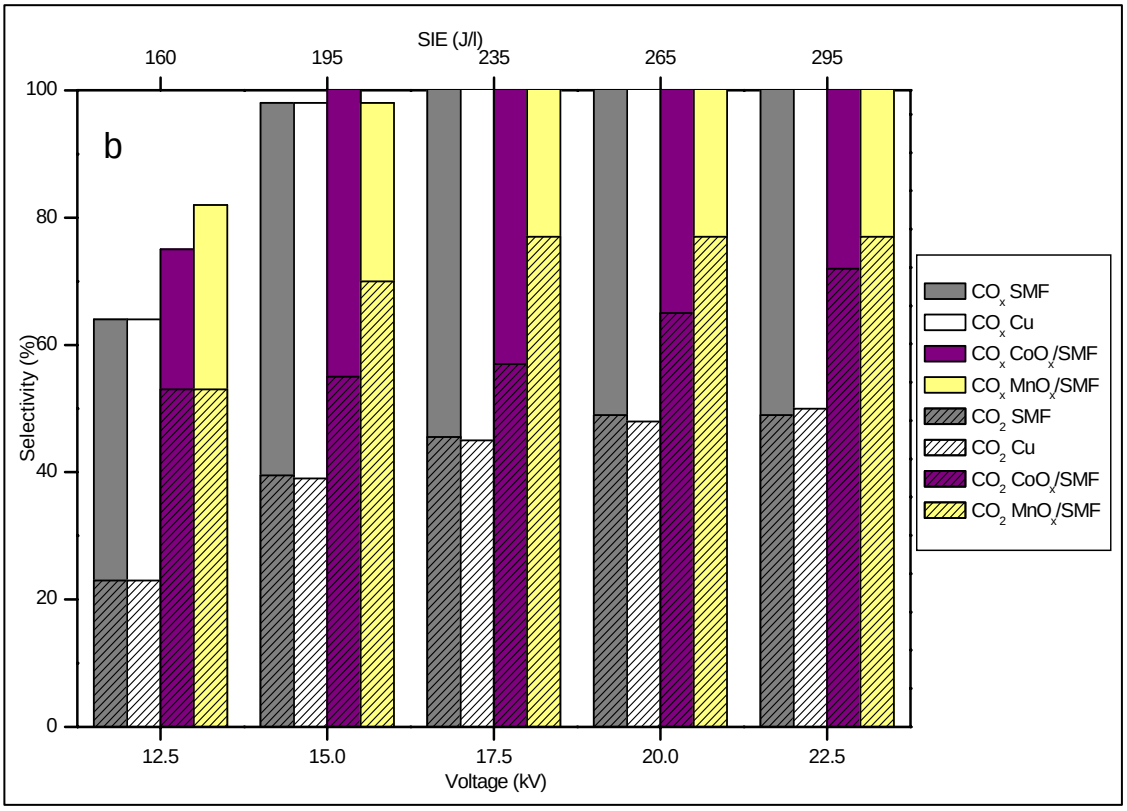
SIE (J/l)
160
195
235
265
295
100
80
60
40
20
0
b
Selectivity (%)
CO$_x$ SMF
CO$_x$ Cu
CO$_x$ CoO$_x$/SMF
CO$_x$ MnO$_x$/SMF
CO$_2$ SMF
CO$_2$ Cu
CO$_2$ CoO$_x$/SMF
CO$_2$ MnO$_x$/SMF
12.5
15.0
17.5
20.0
22.5
Voltage (kV)

Fig. 4a and 4b

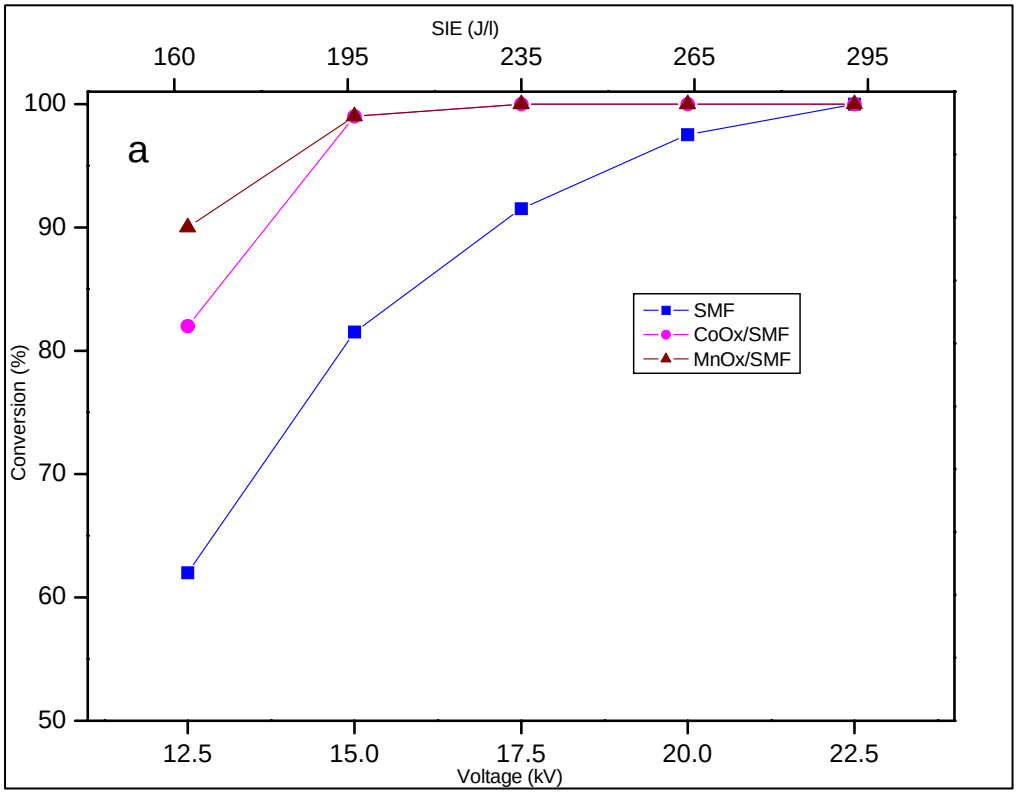
SIE (J/l)
160
195
235
265
295
a
100
90
80
70
60
50
Conversion (%)
SMF
CoOx/SMF
MnOx/SMF
12.5
15.0
17.5
20.0
22.5
Voltage (kV)

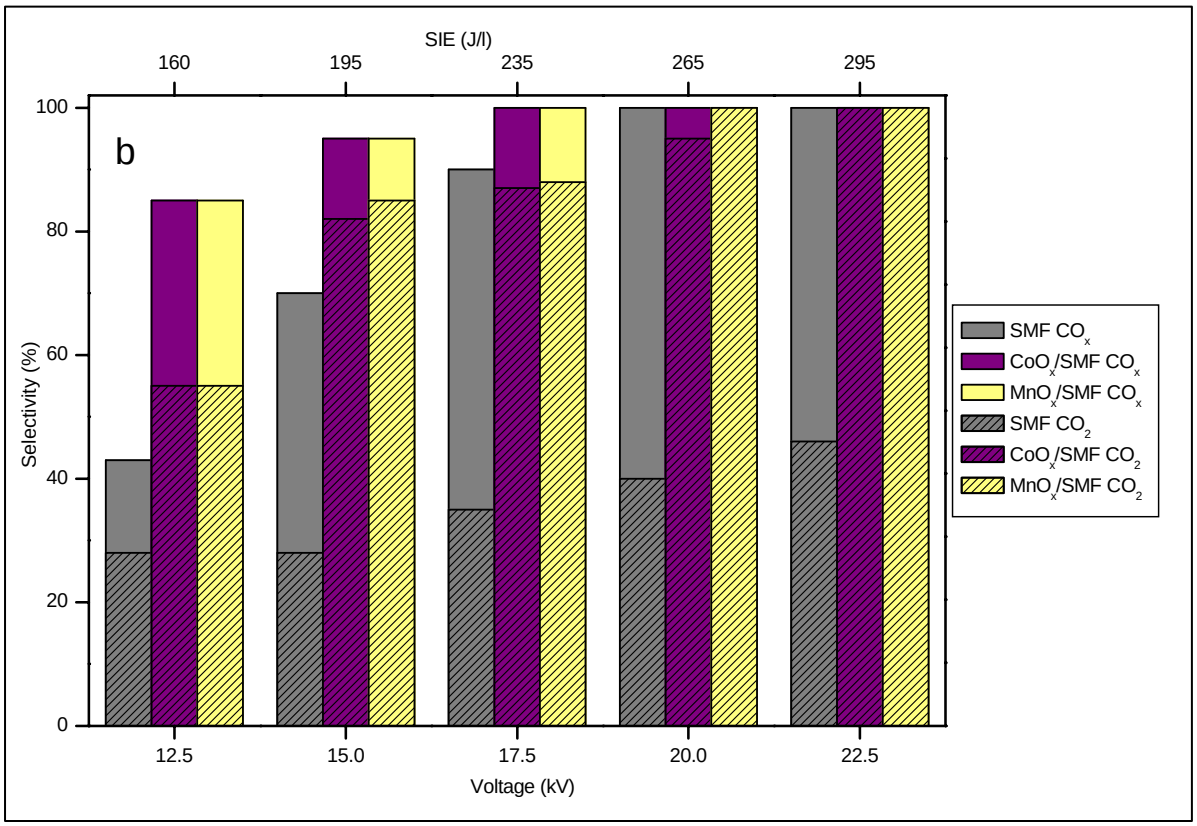
SIE (J/l)
160
195
235
265
295
b
100
80
60
40
20
0
Selectivity (%)
SMF CO$_x$
CoO$_x$/SMF CO$_x$
MnO$_x$/SMF CO$_x$
SMF CO$_2$
CoO$_x$/SMF CO$_2$
MnO$_x$/SMF CO$_2$
12.5
15.0
17.5
20.0
22.5
Voltage (kV)

Fig. 5a and 5b

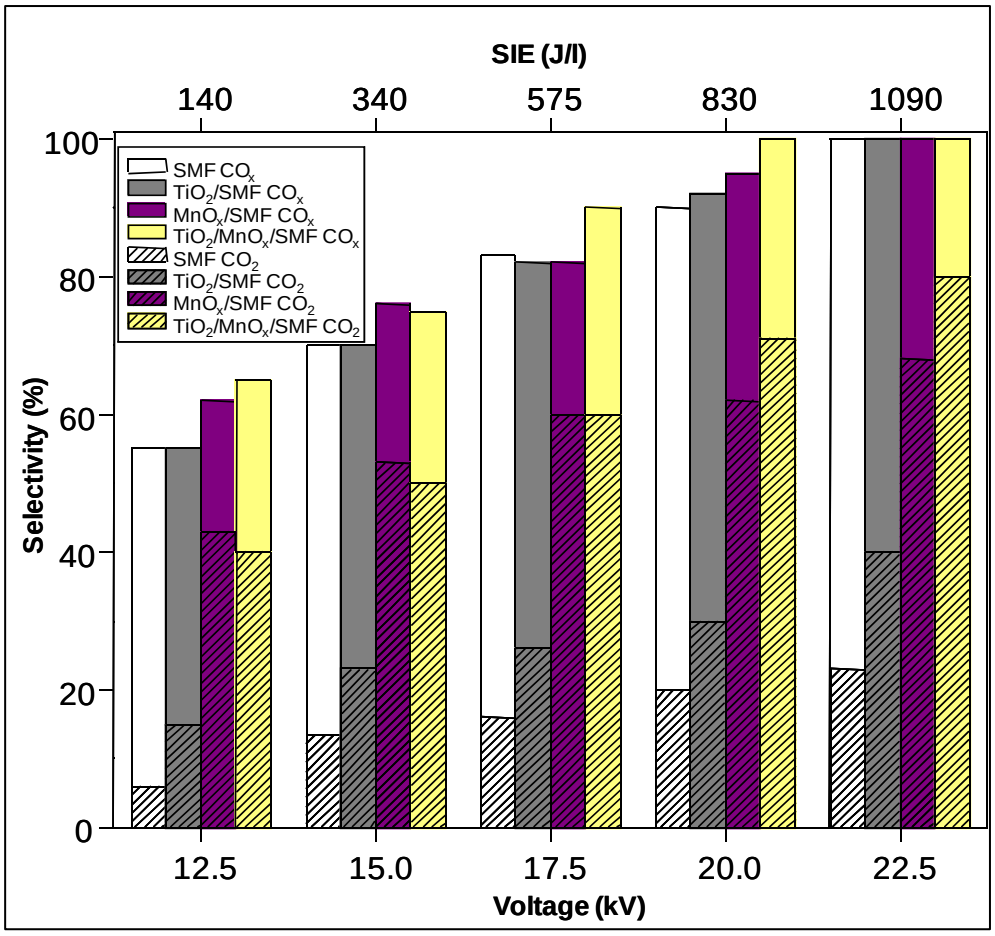
SIE (J/l)
140
340
575
830
1090
100
80
60
40
20
0
Selectivity (%)
SMF CO_x
TiO_2/SMF CO_x
MnO_x/SMF CO_x
TiO_2/MnO_x/SMF CO_x
SMF CO_2
TiO_2/SMF CO_2
MnO_x/SMF CO_2
TiO_2/MnO_x/SMF CO_2
12.5
15.0
17.5
20.0
22.5
Voltage (kV)

Fig. 6